Removal of Barium and Strontium from aqueous solutions: Optimization and modeling

E. A. Motawea; Y. M. moustafa

Analysis and Evaluation Department, Egyptian Petroleum Research Institute, 11727 Nasr City, Cairo, Egypt.

Abstract

Scale formation is recognized as one of the major flow assurance problems affecting production in the oil and gas sector, so removing scale pollutants as Ba^{2+} and Sr^{2+} is of great importance in environmental remediation. An environmentally benign SiO_2-nanoparticles modified EDTA was prepared for treating contaminated water solutions with Ba^{2+} and Sr^{2+}. Adsorption studies were carried out in a binary component system. The Response Surface methodology (RSM) was selected to study and improve the adsorption rate on batch study, and to optimize the most important parameters affecting the adsorption including pH and adsorbent dose. Furthermore, the theoretical constants of kinetic and isotherm of the adsorption were determined in order to more completely understand the Ba^{2+} and Sr^{2+} adsorption mechanism onto adsorbent. Results showed that the adsorption capacities were pH dependent.

Keywords; Scale, Response Surface methodology (RSM), SiO_2-nanoparticles.

INTRODUCTION

In petroleum industries mineral scale formation is a serious and expensive flow assurance challenge for offshore productions, particularly in deep water fields.[1]So researchers must approach methods to produce more oil from the reservoirs that are called enhanced oil recovery (EOR) methods. Water injection is one of the oldest and most commonly used methods as secondary EOR methods in the oilfields. The most frequently used injected water is seawater (SW) because of high quantity and also availability in offshore fields. Injection of SW into the underground oil reservoir is applied in order to displace remaining oil from the reservoirs.

Injected and formation waters (FWs) mix each other and would chemically react with each other, because they contain different types and concentrations of ions resulting incompatible brine . Almost the injected water contains high concentration of the sulfate ions. Also the FW contains almost the high concentration of the cations with two positive charges such as calcium, barium, and strontium ions. This would cause the precipitation of salts that are known as scale precipitates [2]. Inorganic scale deposits (e.g.$CaCO_3$, $BaSO_4$ and $SrSO_4$) can be deposited all along the water paths in the pipeline applications. Oil industries normally encounter two types of scale formation as follows: (1) Carbonate scales ($CaCO_3$ and $FeCO_3$) take place where there is a change in temperature and pressure which results in the release of carbon dioxide from aqueous form to gas form from the flowing fluid. (2) Sulphate scales ($BaSO_4$, $SrSO_4$, $CaSO_4$ and $CaSO_4.H_2O$) come about where there is a mixture of two incompatible brines [3].

Mineral scales form when metal salts exceed their solubility in water under certain temperature and pressure conditions, of many available techniques to control scale formation, chemical treatment utilizing nanoparticles has been widely applied and demonstrated to be successful and economical[4,5].Various methods have been developed to eliminate or reduce the metal ions from aqueous solutions such as chemical precipitation, adsorption electrodialysis and ion exchange, among of all purification methods, the adsorption has been considered as a cost-effective technology[6,7,8].

In this study Response Surface Methodology designed, to optimize the adsorption of Barium and Stronium from aqoues solutions by SiO_2-nanoparticles modified EDTA, Kinetics analyzed to pseudo first-order and pseudo second-order models, also we estimate the equilibrium isotherm constants and their fitness to experimental data using Langmuir, Freundlich. And finally, evaluate thermodynamic parameters to identify the nature of adsorption.

MATERIALS AND METHODS

All reagents used were of analytical purity. Na_2Sio_3 was purchased from Loba chemie. EDTA was obtained from Sigma–Aldrich and used without further purification. Hydrochloric acid, and Ethanol from ADWIC were used. Deionized water was used for preparation of all experimental solutions.

Corresponding author: eman.chemie@gmail.com

Preparation of SiO_2 nanoparticles

The synthesis of SiO_2 nanoparticles was based on the co-precipitation method [9]. A schematic diagram of the synthesis of nano SiO_2 is shown in Fig. 1. 200 ml of deionized water was heated to 80°C under nitrogen flow. Then, a solution of 40 ml $NaSiO_3$ (1M) was added dropwise under vigorous stirring. The pH of the solution was adjusted to 6 with 2M HCL. The reaction was proceeded for 3 hours. Formed nanoparticles were washed with deionized water and alcohol, and then dried in an oven overnight. Finally, nanoparticles were coated with EDTA.

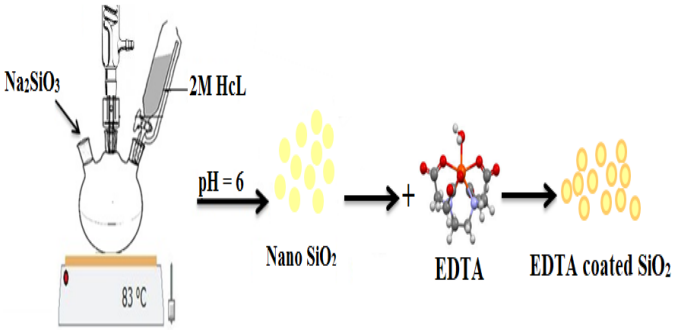

Fig.1. Schematic diagram for the synthesis of nano SiO_2 and coated nano SiO_2.

Characterization of SiO_2 nanoparticles

The infrared spectra of nano SiO_2, and SiO_2 coated EDTA before and after removal of barium and strontium were analyzed using Fourier transform infrared (FTIR) spectroscopy (ATI/Unicam Infinity 961 M instrument) in the range of 4000– 400 cm^{-1}. The size, shape, and distribution of nano SiO_2 were determined by transmission electron microscopy (TEM) (JEOL JEM—2100) at 200 kV. Dynamic light scattering of nano SiO_2 was recorded by Zetasizer Nano-series HT, Malvern instruments. The surface morphology and porous structure nano SiO_2 was examined using scanning electron microscopy (SEM) (JEOL 5410) and the power was set to 30 kV.

Design and optimization of parameters

The effect of adsorption process parameters such as pH and adsorbent dose on the removal efficiency of barium and strontium onto nano SiO_2 was optimized by response surface methodology (RSM) based central composite design (CCD). The CCD model was used to investigate the combination of parameters that will give optimum removal efficiency of Ba^{2+} and Sr^{2+}. Each adsorption parameter has 5 levels designated as $+\alpha$, +1, 0, -1 and $-\alpha$ as shown in Table 1. In the models, dose SiO_2 coated EDTA was varied within 0.002–0.008 mg/20 mL, pH was varied within 4–9. Design expert software (SigmaXL Inc., version 6.23, Canada) was used for statistical data analysis.

Table 1. Experimental factor levels of $NiFe_2O_4$-alginate composite beads

Factors	Levels				
	$-\alpha$	-1	0	+1	$+\alpha$
Adsorbent dose (g/20ml)	0.002	0.005	0.0075	0.008	0.009
pH	4	5	6	8	9

Adsorption studies

The adsorption experiments were performed in a batch mode, at constant temperature 25 °C, stirring rate 150 rpm. Firstly the effects of pH and adsorbent dose on the removal efficiency of Ba^{2+} and Sr^{2+} onto nano SiO_2 modified EDTA was optimized by Response surface methodology. The adsorption behavior was evaluated by Ion Chromatography analysis. The removal percentage of phenol was calculated according to Eq. (1):

$$\text{Adsorption}\ (\%) = \frac{(C_o - C_e)}{C_o} \times 100 \qquad (1)$$

Where, C_o is the initial concentration and C_e is the concentration at equilibrium.

Adsorption kinetics is used to explain the adsorption mechanism of Ba^{2+} and Sr^{2+}, the adsorption data were

treated according to the pseudo-first-order, pseudo-second-order [10, 11] in their linear forms that expressed as:

$$\log(q_e - q_t) = \log(q_e) - (\frac{K_1}{2.303})t \qquad (2)$$

$$\frac{t}{q_t} = \frac{1}{(K_2\, q_e^2)} + \left(\frac{1}{q_e}\right) t \qquad (3)$$

Where, q_t and q_e are the amounts of Ba^{2+} and Sr^{2+} adsorbed at time t and equilibrium e, respectively; K_1 and K_2 are the pseudo first-order and pseudo second-order rate constants, respectively, for the adsorption processes.

Two adsorption isotherm models have been used to analyze the adsorption data by the following equations [12, 13]:

(i) Langmuir.

$$\frac{C_e}{q_e} = \frac{1}{K_L Q_{max}} + \frac{C_e}{Q_{max}} \qquad (4)$$

Where, K_L (L/mg) and Q_{max} (mg/g) are the Langmuir constants related to the adsorption energy and sorption capacity, respectively. While, q_e (mg/g) is the equilibrium adsorption capacity and C_e (mg/L) is the equilibrium concentration.

(ii) Freundlich.

$$\log q_e = \log K_f + \frac{1}{n}\log C_e \qquad (5)$$

Where, K_f (L/mg) is the Freundlich constant and n is the heterogeneity factor which represents sorption capacity and sorption intensity, respectively.

RESULTS AND DISCUSSION

Characterization of SiO_2 nanoparticles

The FTIR of nano SiO_2, SiO_2 modified EDTA and Ba^{2+} and Sr^{2+} loaded SiO_2 modified EDTA are shown in Fig. 2. In the IR spectrum of nano SiO_2 a broad band around 1123 was assigned to asymmetric stretching vibrations of Si-O-Si while the band at 475 was assigned to symmetric stretching. The IR spectrum of SiO_2 modified EDTA exhibited a series of new distinctive changes, where the band around 1123 was shafted to1105.In the spectrum of Ba^{2+} and Sr^{2+} loaded SiO_2 modified EDTA, a decrease in intensity of the band at 1105 was observed and its location shifted significantly to 1050 after Ba^{2+} and Sr^{2+} loading that assigned to carboxylic groups of EDTA participating in Ba^{2+} and Sr^{2+} binding, the decrease and shift in position could also be explained by the relative contribution of SiO_2 in potential Ba^{2+} and Sr^{2+} binding.

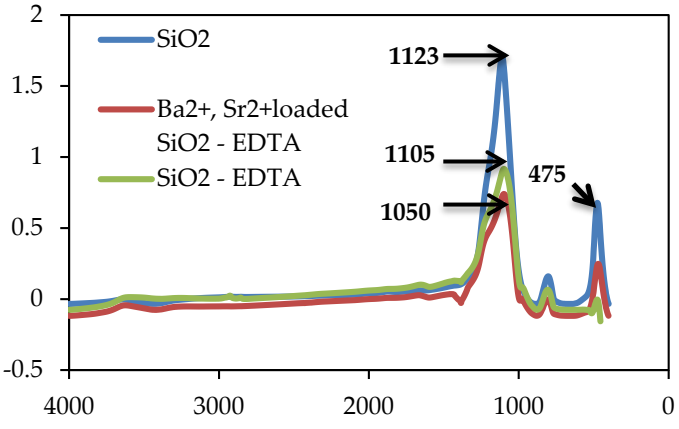

Fig.2. FTIR spectra of: Nano SiO_2, SiO_2 modified EDTA and Ba^{2+} and Sr^{2+} loaded SiO_2 modified EDTA.

The TEM image of the nano SiO_2 particles are shown in Fig. 3. which revealed that the morphology of SiO_2

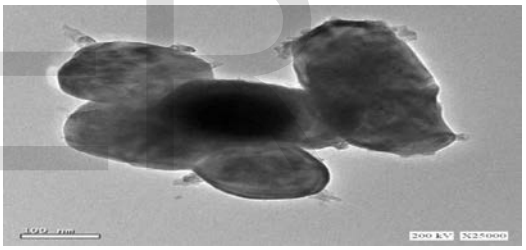

Fig.3. TEM image of nano-SiO_2

nanoparticles were nearly cubic in shape. The DLS characterization of nano SiO_2 particles represented in Fig. 4. showed that the average sizes of nano SiO_2 particles was about 158.5nm.

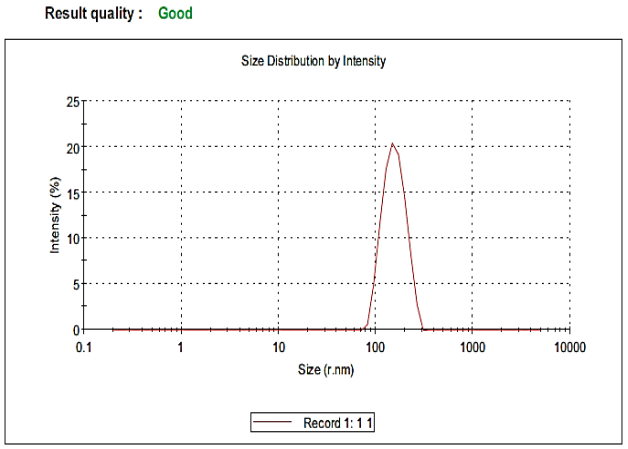

Fig.4. DLS image of nano-SiO2

The SEM micrograph of nano SiO_2particles is shown in Fig. 5, where a relatively homogeneous grain distribution is observed with mainly cubic shape nanoparticles.

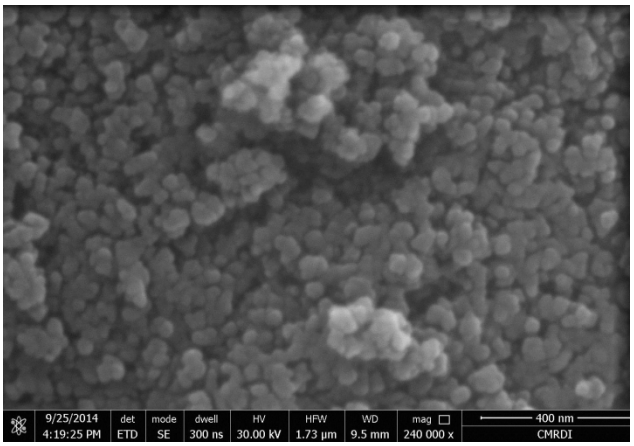

Fig.5. SEM micrograph of nano-SiO_2

Design and optimization

The effect of sorption process parameters such as adsorbent dose and pH on the removal percentage of Ba^{2+} and Sr^{2+} onto SiO_2 modified EDTA was investigated using central composite design (CCD), which is a statistical and mathematical technique useful for building models, designing experiments and analyzing the interactive effects of several independent parameters. The main advantage of CCD is to reduce the number of experiments to be conducted, to study the interactions of operations parameters and to optimize the adsorption conditions [16,17].

Table 2.ANOVA analysis of response surface for removal of Ba^{2+} and Sr^{2+} using SiO_2 modified EDTA

Adsorbate	Source	DF	SS	MS	F-value	Prob.> F
Barium (Ba^{2+})	Model	5	1889.5	377.90	3.156	0.0411
	Error	4	478.91	119.73	-	-
	Lack of Fit	3	478.41	159.47	318.94	0.1441
	Pure Error	1	0.5000	0.5000	-	-
	Total (Model + Error)	9	2368.4	263.16	-	-
Strontium (Sr^{2+})	Model	5	1794.0	358.79	4.434	0.0370
	Error	4	323.65	80.912	-	-
	Lack of Fit	3	321.65	107.22	53.608	0.07000
	Pure Error	1	2	2	-	-
	Total (Model + Error)	9	2117.6	235.29	-	-

The results for the ANOVA of the response surface quadratic analyses and model terms are summarized in Table 2. The high coefficient of determination value for Ba^{2+} and Sr^{2+} (R^2 = 0.98, 0.96 respectively) showed that the quadratic modes utilized highly sufficient in predicting the responses. Also, the F-value of 3.15 and 4.43, respectively, of the quadratic model implied that the equation was significant. The values of probability > F was 0.0411 and 0.0370 respectively, showed model terms were significant. From the model, the predicted Ba^{2+} and Sr^{2+} removal and optimum conditions by SiO_2 modified EDTA (adsorbent dose: 9 mg/ 20 mL and pH 5.0) with predicted Ba^{2+} and Sr^{2+} percent removal 60.5% and 64% respectively, were obtained. While, the actual Ba^{2+} and Sr^{2+} percent removal were 59% and 63%, respectively, this indicated the reliability of the models. Fig. 6(a and b) indicated 3D response surface plots of percent removal of Ba^{2+} and Sr^{2+} as a function of two adsorption parameters.

From the model, the predicted Ba^{2+} and Sr^{2+} removal and optimum conditions was (adsorbent dose: 9 mg/ 20 mL and pH 5.0) .

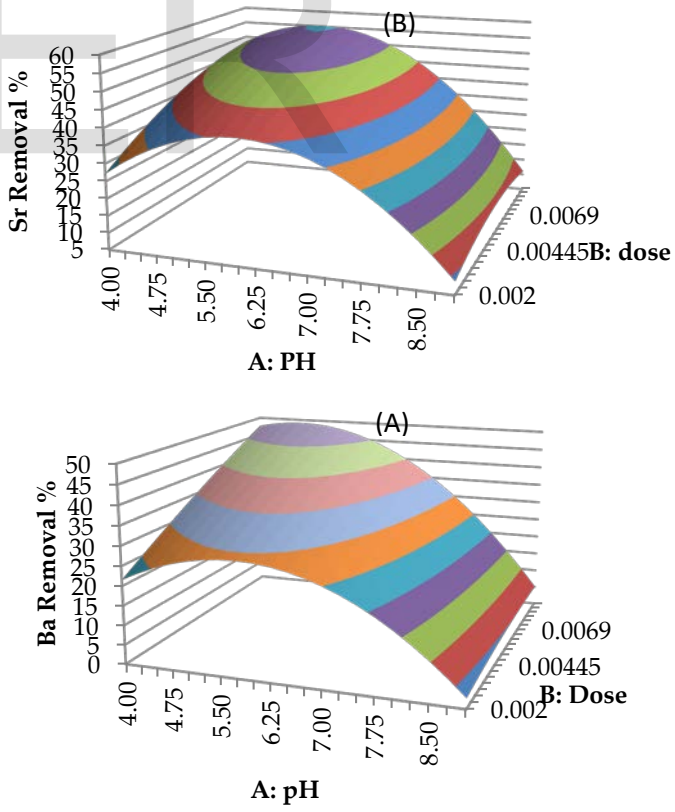

Fig.6. 3D Response surface plot for the combined effect of pH with the effect of adsorbent dose on the removal % of (A) Ba^{2+} and (B) Sr^{2+} by SiO_2 modified EDTA.

Kinetics and adsorption mechanism of Ba^{2+} and Sr^{2+}

The adsorption of Ba^{2+} and Sr^{2+} onto SiO_2 modified EDTA as a function of time was treated by pseudo-first-order and pseudo-second-order (Fig. 7) models. The pseudo-first-order and pseudo-second-order rate constants as well as equilibrium sorption capacities are reported in Table 3.

The graph revealed that the sorption kinetics of Ba^{2+} and Sr^{2+} onto SiO_2 modified EDTA followed the pseudo-second-order model and the correlation coefficient (R^2) for linear plots of t/qt against time were 0.9972 and 0.9985 for Ba^{2+} and Sr^{2+} respectively, suggesting that the sorption obeys the pseudo-second-order model. Such a model assumes that the rate limiting step may be governed by chemisorption involving valence forces through sharing or exchanging electrons between sorbent and sorbate[18,19], and the adsorption governed by an ion-exchange mechanism.

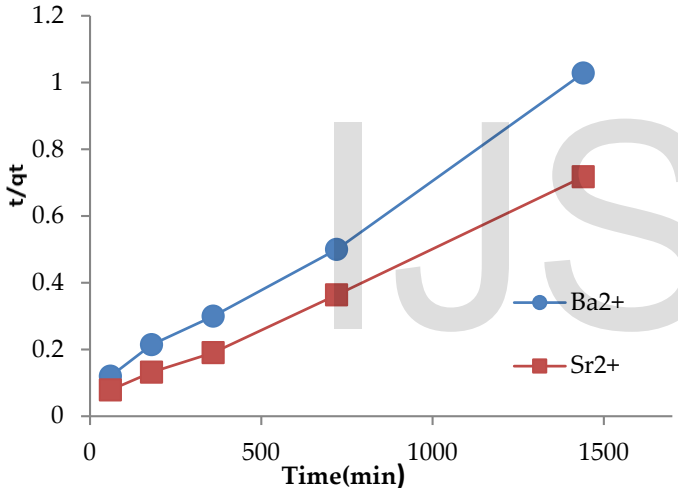

Fig.7. Adsorption kinetics of pseudo-second order for the adsorption of Ba^{2+} and Sr^{2+} onto SiO_2 modified EDTA (adsorbent dosage 9 mg/20 mL, initial Ba^{2+} and Sr^{2+} ion concentration 1500 µmol/L and temperature 25°C).

Table3. Kinetic parameters of the pseudo-first and second-order models for the adsorption of Ba^{2+} and Sr^{2+} onto SiO_2 modified EDTA (adsorbent dosage 9 mg/20 mL, initial Ba^{2+} and Sr^{2+} ion concentration 1500 µmol/L and temperature 25°C).

Adsorbate	Kinetic model	Kinetic constants				
		R^2	K_1(min^{-1})	$q_{e,cal}$ (mol/g)	K_2(g/mg min)	$q_{e,cal}$ (mol /g)
Ba^{2+}	Pseudo-first order	0.579	0.00414	566.63		
	Pseudo-second order	0.997			0.0000042	1453.61
Sr^{2+}	Pseudo-first order	0.812	0.00506	1228		
	Pseudo-second order	0.998			0.0000063	1900.45

Ba^{2+} and Sr^{2+} adsorption isotherm

Adsorption isotherms are used to describe the relationship between the mass of metal adsorbed per unit mass of adsorbent and the aqueous phase metal concentration at equilibrium and constant temperature [20,21].The equilibrium data were analyzed using the Langmuir and Freundlich isotherm models Eqs. (4) and (5). The Langmuir model assumes that the adsorption occurs on a homogeneous surface by monolayer coverage with uniform binding sites, equivalent sorption energies, and no interactions between adsorbed species. While, the Freundlich isotherm is an empirical equation assuming that the adsorption process takes place on heterogeneous surfaces and adsorption capacity is related to the concentration of the adsorbate at equilibrium [22,23]. A comparison of the fit of the Langmuir and Freundlich equations of Sr^{2+} and Ba^{2+} sorption by SiO_2 modified EDTA are shown in Figs. 8 and 9, respectively. Also, their constants along with correlation coefficients (R^2) are depicted in Table 4.

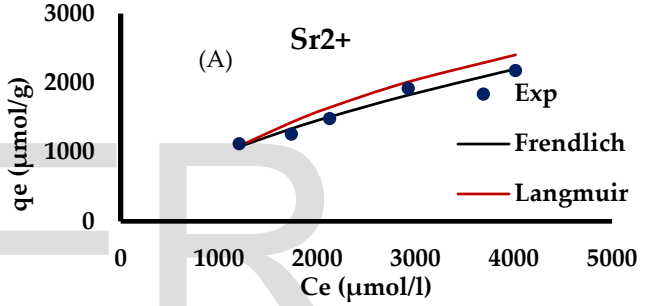

Fig.8. (A)Comparison of the fit of the Langmuir and Freundlich isotherm models for the adsorption of Sr^{2+} onto SiO_2 modified EDTA (adsorbent dosage 9 mg/20 mL, contact time 1440 min and temperature 25 °C).

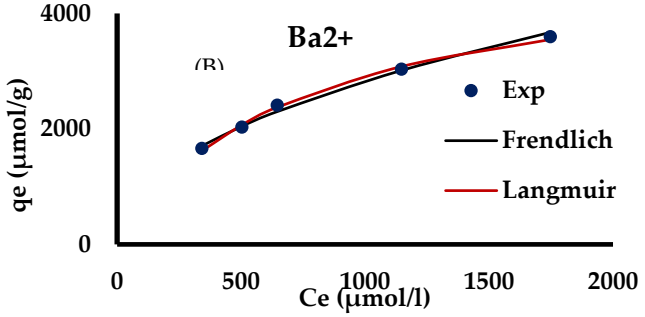

Fig.8. (B)Comparison of the fit of the Langmuir and Freundlich isotherm models for the adsorption of Ba^{2+} onto SiO_2 modified EDTA (adsorbent dosage 9 mg/20 mL, contact time 1440 min and temperature 25 °C).

The results revealed that in the binary system, the adsorption capacities of Sr^{2+} and Ba^{2+} in close agreement with the theoretical prediction of Freundlich and Langmuir models. In the multicomponent system, the adsorption is complicated because the interactions between solutes are involved. In the bi-solute systems, factors that affect the adsorption preference of an adsorbent for metal cations may be related to the characteristics of the adsorbent and the properties of the metal cation such as coordination

number, ionic size, standard reduction potential and Pauling electronegativity [6].The more electronegative metal ion will be more attracted to the surface of SiO_2. Barium has the lowest sorption capacity and the lowest electronegativity. The ratio of standard reduction potential to ionic radius can be considered as a suitable criterion for predicting relative sorption capacity, therefore, Sr^{2+} ions (the least diameter) have maximum adsorption and Ba^{2+} ions (the biggest diameter) have minimum adsorption[6].

Table4.Adsorption isotherm parameters of Langmuir and Freundlich models for the adsorption of Ba^{2+} and Sr^{2+} (adsorbent dosage 9 mg/20 mL, initial Ba^{2+} and Sr^{2+} ion concentration 1500,2500, 3500, 4500 and 5500 µmol/L, contact time 1440 min and temperatures of 25 °C)

Adsorbent	Isotherm model	Isotherm constants				
		R^2	Qmax	b	Kf	1/n
Ba^{2+}	Langmuir	0.954	4545	0.00025		
	Freundlich	0.97			16.01	0.59
Sr^{2+}	Langmuir	0.926	5000	0.00051		
	Freundlich	0.9729			40.02	0.5424

CONCLUSION

The removal of Ba^{2+} and Sr^{2+} from aqueous solutions by SiO_2 modified EDTA has been investigated here. The optimum conditions obtained by response surface methodology were pH of 5.0 and adsorbent dose of 9 mg/20 mL of SiO_2 modified EDTA. The adsorption kinetics was best described by the pseudo-second-order model and the adsorption isotherm was described by both Langmuir and Freundlich adsorption. The maximum adsorption capacities were 4545 and 5000 µmol /g for Ba^{2+} and Sr^{2+}, respectively. These cations was adsorbed in the following selectivity sequence Sr^{2+}> Ba^{2+}.

REFERENCES

[1] P. Zhang, T. Kan and B. Tomson, Enhanced transport of novel crystalline calcium phosphonate scale inhibitor nano materials and their long term flow back performance in laboratory squeeze simulation tests, RSC Adv., 6, (52), (2016), 59-71.

[2] A. Golsefatan, M. Safari & M. Jamialahmadi, Using silica nanoparticles to improve DETPMP scale inhibitor performance as a novel calcium sulfate inhibitor, Desalination and Water Treatment,4, (2015) 1–9.

[3] M. Vazirian, T. Charpentier, M. Penna, A. Neville, Surface inorganic scale formation in oil and gas industry: As adhesion and deposition processes, Journal of Petroleum Science and Engineering, 137(2016)22–32.

[4] P. Zhang, G. Ruan, T. Kan and B. Tomson, Functional scale inhibitor nanoparticle capsule
delivery vehicles for oilfield mineral scale control, RSC Adv., 6, (2016),43-56.

[5] P. Zhang, C. Fan, H. Lu, T. Kan, and B. Tomson, Synthesis of Crystalline-Phase Silica-Based Calcium Phosphonate Nanomaterials and Their Transport in Carbonate and Sandstone Porous Media, Ind. Eng. Chem. Res. 50, (2011),1819–1830.

[6] M. Araissi, I. Ayed, E. Elaloui and Y. Moussaoui, Removal of barium and strontium from aqueous solution using zeolite 4A, Water Science & Technology, 73, (2016),1628-1636.

[7] A. Bakr, Y. Moustafa, E.Motawea, M. Yehia, M.H. Khalil, Removal of ferrous ions from their aqueous solutions onto NiFe2O4–alginate composite beads, Journal of Environmental Chemical Engineering, 3, (2015) 1486–1496.

[8] A. Bakr, Y. Moustafa, E.Motawea, M. Yehia, M.H. Khalil, Magnetic nanocomposite beads: synthesis and uptake of Cu(II) ions from aqueous solutions, Can. J. Chem. 93, (2015),289-299.

[9] S. Musić1, N. F. Vinceković and L. Sekovanić, PRECIPITATION OF AMORPHOUS SiO2 PARTICLES AND THEIR PROPERTIES, Brazilian Journal of Chemical Engineering,28, (2011),89-94.

[10] A. Morsy, M. El-Sheikh, A. Barhoum, Nano-silica and SiO2/CaCO3 nanocomposite
prepared from semi-burned rice straw ash as modified papermaking fillers, Arabian Journal of Chemistry,8, (2014),123-134.

[11] M. Bhaumik, T.Leswifi, A. Maity, V. Srinivasu, S. Onyango, Removal of fluoride from aqueous solution by polypyrrole/Fe3O4 magnetic nanocomposite, Journal of Hazardous Materials 186 (2011) 150–159.

[12] W. Ngah , S. Ghani, A. Kamari, Adsorption behaviour of Fe(II) and Fe(III) ions in aqueous solution on chitosan and cross-linked chitosan beads, Bioresource Technology, 96, (2005), 443–450.

[13] X. Li, Y. Qi, Y. Li , Y. Zhang, X. He, Y. Wang, Novel magnetic beads based on sodium alginate gel cross linked by zirconium(IV) and their effective removal for Pb2+ in aqueous

solutions by using a batch and continuous systems, Bioresource Technology, 142, (2013), 611–619.

[14] A.Kul, H. Koyuncu, Adsorption of Pb(II) ions from aqueous solution by native and activatedbentonite: Kinetic, equilibrium and thermodynamic study, Journal of Hazardous Materials, 179, (2010), 332–339.

[15] M. Bhaumik, T.Leswifi, A. Maity, V. Srinivasu, S. Onyango, Removal of fluoride from aqueous solution by polypyrrole/Fe3O4 magnetic nanocomposite, Journal of Hazardous Materials 186 (2011) 150–159.

[16] B. Kiran, K. Thanasekaran, Copper biosorption on Lyngbya putealis: application of response surface methodology (RSM), Int. Biodeterior. Biodegrad. 65 (6) (2011) 840–845, doi:http://dx.doi.org/10.1016/j.ibiod.2011.06.004.

[17] R. Myers, D. Montgomery, C. Anderson, Response Surface Methodology: Process and Product Optimization Using Designed Experiments, 3rd ed., Wiley Series in Probability and Statistics, New Jersey, 2009.

[18] A.F. Hassan, A.M. Abdel-Mohsen, M.M. Fouda, Comparative study of calcium alginate, activated carbon, and their composite beads on methylene blue adsorption, Carbohydr. Polym. 102 (2014) 192–198, doi:http://dx.doi.org/ 10.1016/j.carbpol.2013.10.104. 24507272.

[19] S. Rengaraj, J.W. Yeon, Y. Kim, Y. Jung, Y.K. Ha, W.H. Kim, Adsorption char- acteristics of Cu(II) onto ion exchange resins 252H and 1500H: kinetics, isotherms and error analysis, J. Hazard. Mater. 143 (1–2) (2007) 469–477, doi: http://dx.doi.org/10.1016/j.jhazmat.2006.09.064.

[20] G. Limousin, J.- Gaudet, L. Charlet, S. Szenknect, V. Barthès, M. Krimissa, Sorption isotherms: a review on physical bases, modeling and measurement, Appl. Geochem. 22 (2) (2007) 249–275, doi:http://dx.doi.org/10.1016/j. apgeochem.2006.09.010.

[21] T. Petrova, L. Fachikov, J. Hristov, The magnetite as adsorbent for some haz-ardous species from aqueous solutions: a review, Int. Rev. Chem. Eng. 3 (2) (2011) 134–152.

[22] A.A. Bakr, M.S. Mostafa, G. Eshaq, M.M. Kamel, Kinetics of uptake of Fe(II) from aqueous solutions by Co/Mo layered double hydroxide (Part 2), Desalin. Water Treat. (2014) 1–8, doi:http://dx.doi.org/10.1080/19443994.2014.934729.

[23] G. Limousin, J.- Gaudet, L. Charlet, S. Szenknect, V. Barthès, M. Krimissa, Sorption isotherms: a review on physical bases, modeling and measurement, Appl. Geochem. 22 (2) (2007) 249–275, doi:http://dx.doi.org/10.1016/j. apgeochem.2006.09.010.